Frustration and inhomogeneous environments in relaxation of open chains with Ising-type interactions

D. Valente* and T. Werlang†
Instituto de Física, Universidade Federal de Mato Grosso, CEP 78060-900, Cuiabá, MT, Brazil

(Received 20 April 2020; accepted 21 July 2020; published 10 August 2020)

Frustration can contribute to very slow relaxation times in large open chains, as in spin glasses and in biopolymers. However, frustration may not be sufficient to produce broken ergodicity in finite systems. Here we employ a system-plus-reservoir approach to investigate how strongly inhomogeneous environments and frustration compete in the relaxation of finite open chains. We find a sufficient condition for our inhomogeneous environments to break ergodicity. We use the microscopic model to derive a Markovian quantum master equation for a generic chain with ultrastrong intrachain couplings. We show that this microscopic model avoids a spurious broken ergodicity we find in the phenomenological model. We work out an explicit example of broken ergodicity due to the inhomogeneous environment of an unfrustrated spin chain as far as simulating a recent experiment on protein denaturation (where environment inhomogeneity is especially relevant). We finally show that an inhomogeneous environment can mitigate the effects of frustration-induced degeneracies.

DOI: 10.1103/PhysRevE.102.022114

I. INTRODUCTION

In a frustrated system, no configuration exists that simultaneously minimizes all its energetic contributions [1]. Frustration can create multiple low-energy metastable states, leading to very slow relaxation times. Such a slow relaxation can effectively trap the system in a subset of all possible states, breaking ergodicity on experimentally accessible timescales. Magnetic frustration, when combined with intrinsic disorder, can give rise to a spin glass, an emblematic example of broken ergodicity [1–3]. Frustration can also affect the folding of biopolymers in living organisms [4,5]. Proteins, for instance, are large sequences of aminoacids that relax from an unfolded to a final state. In biologically functional proteins, final states are those folded in specific, compact geometries, called native states. From the physics viewpoint, this protein relaxation dynamics is understood as diffusion in a rugged funneled energy landscape, and the native states occupy the lowest energy subspace, i.e., the bottom of the funnel [6,7]. Randomly chosen aminoacid sequences are unable to fold to its most compact, less energetic state. Frustration, in this case, blocks the protein from finding a single well-isolated folded structure of minimum energy [8].

However, frustration may not be sufficient to produce broken ergodicity. Barriers between the multiple energy states of the system may not be high enough [1]. The question that interests us here is how specific system-environment interactions contribute to the relaxation of open chains and to break ergodicity [9–14], and what kind of interplay with frustration [15,16] there can be found.

The system-plus-reservoir approach for open quantum systems [17,18] turns out to be well adapted to address this problem for finite chains. This approach sets a global Hamiltonian (allowing for quantization of both the system and the environment) that reproduces the stochastic dynamics of the quantum system of interest. Most importantly here, the explicit Hamiltonian formulation allows us to consider both frustration and environmental effects in a consistent manner. Historically, the system-plus-reservoir approach has provided us with microscopic quantum theories for paradigmatic irreversible processes, such as the spontaneous emission of a photon by a single atom [19], the decay of magnetic flux in a superconducting artificial atom [20] and quantum decoherence due to phonon baths in semiconducting artificial atoms [21]. More recently, derivation of quantum master equations for weak system-bath couplings have allowed the investigation not only of relaxation of quantum chains [13], but also of heat transport between multiple reservoirs at different temperatures [22–29]. The so-called microscopic model for the master equation has been shown particularly useful for describing heat transport in the ultrastrong intrachain couplings regime [24–26].

Here we employ the system-plus-reservoir approach to investigate how an inhomogeneous environment (i.e., an inhomogeneous distribution of system-reservoir couplings along a finite quantum chain) competes with frustration in the relaxation of the chain. Inhomogeneous environments are expected to affect both naturally occurring and engineered chains [30–33]. We derive a Markovian quantum master equation within the microscopic model, valid for ultrastrong intersite couplings. We first discuss a sufficient condition for our inhomogeneous environments to break ergodicity. Then we turn our attention to key examples in spin chains. We devise a case to highlight why the microscopic model is necessary to suitably describe relaxation in a frustrated spin chain, avoiding spurious effects from the phenomenological model. We then find an example where a completely unfrustrated

*valente.daniel@gmail.com
†thiago.werlang80@gmail.com

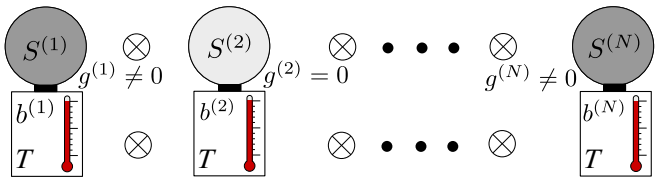

FIG. 1. Model of the system-reservoir couplings. The system, with Hamiltonian H_S and state $\rho_S(t)$, consists of a chain of degrees of freedom locally coupled, via operators $S^{(n)}$ and strengths $g^{(n)}$, to independent reservoir modes $b^{(n)}$, all at the same temperature T. We are interested in the interplay between an arbitrary distribution of couplings $g^{(n)}$ (in H_{SR}) and frustration (in H_S) to the chain's relaxation.

spin chain cannot attain its lowest energy levels due to the strong inhomogeneity of the environment. We explore this as far as simulating a recent experiment on protein denaturation [34]. Our motivation is that spatial inhomogeneity of a protein's environment strongly affects the difference between thermal and chemical denaturation [35], as evidenced by the so-called molecular transfer model [36–40]. We finally find an example where inhomogeneity can induce relaxation to a single state, among three nearly degenerate lowest-energy levels of a frustrated chain. In this sense, the effect of frustration gets mitigated by the inhomogeneous environment. Our results contribute to the understanding of out-of-equilibrium dynamics of many-body open quantum systems by developing a method that treats relaxation [11,12,14] consistently with frustration [15,16].

II. MODEL

We label as H_S the Hamiltonian of a generic isolated quantum system. The only assumption we need to make at this point is that we know its spectral decomposition,

$$H_S = \sum_{j=1}^{d} E_j |j\rangle\langle j|, \tag{1}$$

where d is the size of the Hilbert space. Once the Hamiltonian of the chain is diagonalized, our theory can describe both harmonic [23,29] and spin chains, comprising the Ising model with tilted fields, the XY model, the XXZ model, and the Heisenberg model [11,12,16,28,33]. Following the system-plus-reservoir approach, the Hamiltonian of the system coupled to its environment is set to $H = H_S + H_{SR} + H_R$. We model the reservoir Hamiltonian $H_R = \sum_{n=1}^{N}\sum_k \hbar\omega_k^{(n)} b_k^{(n)\dagger} b_k^{(n)}$ as a finite set of N independent baths, each consisting of quantum harmonic modes b_k of frequencies ω_k (which will be treated in the continuum limit, $\sum_k \to \int dk$). Let us consider that each independent bath is locally coupled to a distinct degree of freedom $S^{(n)}$ of the system, as described by (see Fig. 1)

$$H_{SR} = \sum_{n=1}^{N} S^{(n)} \otimes \sum_k \hbar g_k^{(n)} \left(b_k^{(n)\dagger} + b_k^{(n)}\right). \tag{2}$$

In the case where the system is a spin-1/2 chain, for instance, $S^{(n)}$ may represent a Pauli operator, whereas in harmonic chains, $S^{(n)}$ may represent the bosonic operator of the nth oscillator. For N spins-1/2, we have that $d = 2^N$. Our model in Eq. (2) generalizes the system-environment Hamiltonians considered in Refs. [9,10,13].

We describe the state of our general quantum system by its density matrix, $\rho_S(t)$. Our goal is to establish the quantum master equation governing the dynamics of $\rho_S(t)$. To that end, we proceed by tracing out the environmental degrees of freedom from the complete quantum state evolved unitarily, $\rho_S(t) = \mathrm{Tr}_R[U\rho(0)U^\dagger]$, where $U = \exp(-iHt/\hbar)$, from an initially uncorrelated global state $\rho(0) = \rho_S(0)\otimes\rho_R(0)$. We choose a thermal equilibrium state for the reservoir at temperature T, so that $\rho_R(0) = \exp(-\beta H_R)/Z_R$, with $\beta = 1/(k_B T)$, where k_B is the Boltzmann's constant and $Z_R = \mathrm{Tr}[\exp(-\beta H_R)]$ is the partition function. We assume perturbative system-reservoir couplings up to second order. This allows us to characterize the couplings between each degree of freedom of the system to its local reservoir by the so-called spectral function $J^{(n)}(\omega) = 2\pi\sum_k |g_k^{(n)}|^2 \delta(\omega - \omega_k^{(n)})$, which is well defined in the continuum limit, $\sum_k \to \int dk$. These steps lead to the derivation of a Markovian quantum master equation for the system density operator in the so-called Lindblad form [17],

$$\partial_t \rho_S(t) = -(i/\hbar)[H_S, \rho_S(t)] + L[\rho_S(t)], \tag{3}$$

where $L[\rho_S(t)]$ supports the relaxation effects we wish to explore. It reads

$$L[\rho_S] = \sum_{n=1}^{N}\sum_{\omega>0} J^{(n)}(\omega)(1+\bar{n}_\omega)\left[A_\omega^{(n)}\rho_S A_\omega^{(n)\dagger} - \frac{1}{2}\left\{\rho_S, A_\omega^{(n)\dagger}A_\omega^{(n)}\right\}\right] + J^{(n)}(\omega)\,\bar{n}_\omega\left[A_\omega^{(n)\dagger}\rho_S A_\omega^{(n)} - \frac{1}{2}\left\{\rho_S, A_\omega^{(n)}A_\omega^{(n)\dagger}\right\}\right], \tag{4}$$

where $\omega = \omega_{ij} = (E_j - E_i)/\hbar > 0$, the average number of excitations is $\bar{n}_\omega = [\exp(\beta\hbar\omega) - 1]^{-1}$, as given by the Bose-Einstein distribution, and the jump operators are defined by

$$A_\omega^{(n)} = \sum_{i,j|\omega=\omega_{ij}} |i\rangle\langle i|S^{(n)}|j\rangle\langle j|. \tag{5}$$

Operators $A_\omega^{(n)}$ are valid for both nondegenerate and degenerate gaps. The generalization of Eq. (4) for degenerate spectra ($\omega \to 0$) can be found by following Refs. [17,25].

The jump operators $A_\omega^{(n)}$ evidence the fundamental aspect retained by this microscopic approach, in that the bath acts locally, via $S^{(n)}$, and affects globally, given that $|j\rangle$ is an eigenstate of the entire system. In contrast with Eq. (5), the phenomenological approach employs jump operators that induce transitions between the eigenstates of each subsystem, motivated by regimes of weak intersite couplings [17]. Let us take, for instance, the case of a spin-1/2 chain and choose $S^{(k)} = \sigma_x^{(k)}$ for a given (k). In this case, the phenomenological approach would typically employ jump operators in the form

$$A_{\mathrm{ph}}^{(k)} = |{\downarrow}\rangle\langle{\downarrow}|\sigma_x^{(k)}|{\uparrow}\rangle\langle{\uparrow}| = \sigma_-. \tag{6}$$

In general, $A_{\mathrm{ph}}^{(n)} \neq A_\omega^{(n)}$ for composite systems (for instance, $\langle{\downarrow\downarrow}|\sigma_x^{(1)}|{\uparrow\uparrow}\rangle = 0$, whereas $\langle{\downarrow}|\sigma_x^{(1)}|{\uparrow}\rangle = 1$). As far as heat

transport is concerned, microscopic and phenomenological approaches generally imply distinct theoretical predictions, which has been the subject of intense controversies [23,24,26–29]. As far as relaxation is concerned (the central issue here), the microscopic model, Eq. (4), appropriately guarantees that the Gibbs state $\rho_S(\infty) = \exp(-\beta H_S)/Z_S$ is one (not necessarily unique) steady-state solution for the open system dynamics. In the cases we have checked, the phenomenological approach has led instead to a state $\propto \exp(-\beta \sum_\alpha H_\alpha)$, where H_α is the free Hamiltonian for the αth degree of freedom alone, i.e., $\sum_\alpha H_\alpha \neq H_S$. We will return to this discussion further in this paper (see Sec. IV A). It is important to emphasize that our approach here bridges the gap between recent discussions on relaxation [11,12,14] and on frustration [15,16] of open quantum spin chains, since we explicitly consider the system's Hamiltonian H_S both to identify frustration and to compute relaxation rates, as shown in Eq. (5).

III. RESULTS FOR GENERAL N

A. Relaxation of general inhomogeneously open chains: Breaking ergodicity

We now establish our most general result, namely, a sufficient condition for an inhomogeneous reservoir to break ergodicity, even in the complete absence of frustration in the system's Hamiltonian. As we try to make clear below, these general conditions have all the same origin, that is, the nonuniqueness of the steady state $\rho_S(\infty)$ under inhomogeneous reservoir couplings along an open chain. The relevant properties of $\rho_S(t)$ emerge when we rewrite it as a column vector $\vec{\rho}_S$. We recast the master equation (3) in the form

$$\partial_t \vec{\rho}_S = \Lambda \vec{\rho}_S, \tag{7}$$

where Λ is a time-independent square matrix representing the transition rates between all the elements of $\rho_S(t)$. We are interested, in this section, in the more typical case where the system's spectrum is nondegenerate. A nondegenerate spectrum implies that the quantum coherences decouple from the populations [17], allowing us to only focus on the latter, $(\vec{\rho}_S)_i = \langle i|\rho_S|i\rangle$. Now Λ_{ij} becomes the transition rate only between the energy eigenstates $|j\rangle \to |i\rangle$. Equation (7) then simply becomes the Pauli master equation. We arrive here at a sufficient condition for ergodicity breaking: a block diagonal Λ (in some order) implies a set of decoupled energy subspaces. The stationary state is not unique and it depends on the system's initial state, when Λ is block diagonal. Our block diagonal Λ (comprising the whole set $\{S^{(n)}\}$) generalizes the block-diagonal structure of the single-operator matrix $\langle i|S|j\rangle$ from Ref. [13], where constants of motion are discussed. If the system has a finite probability of being initially excited with a certain energy outside the lowest-energy subspace, the relaxation pathway from the higher-energy to the lowest-energy subspace will be forbidden. The excited portion of the ensemble will be blocked from attaining the state of minimum energy, no matter how low the temperature is set. It shows how an inhomogeneous bath can replace the role played by frustration in preventing open chains to achieve its minimum energy states. The opposite pathway, that would lead to excitation, is also forbidden. If the system starts trapped within a given low-energy subspace, there it will remain no matter how high the temperature is set. The only mechanism that allows it to escape, as to achieve higher energy configurations, is by turning on the coupling between a degree of freedom and its local environment (breaking the block-diagonal structure of Λ, in our theory). This distinction between exciting the chain by increasing the temperature T in contrast to increasing a local coupling $J^{(n)}(\omega)$ reminds us of the difference between thermal and chemical denaturations in proteins, as further explored in the following section.

In order to establish how the distribution of couplings along the chain generates the desired decoupled subspaces [in other words, how $J^{(n)}(\omega)$ creates a block diagonal Λ], we need an explicit form for Λ. We add another simplifying condition, that the gaps ω_{ij} are also nondegenerate [the expression for $A^{(n)}_\omega$ in Eq. (5) is readily suitable to treat degenerate gaps as well]. We find that

$$\Lambda_{ii} = \Gamma^{(0)}_i, \quad \Lambda_{i<j} = \Gamma^{(D)}_{ij}, \quad \text{and} \quad \Lambda_{i>j} = \Gamma^{(G)}_{ij}. \tag{8}$$

Consistently with Fermi's golden rule [17], the off-diagonal elements here read

$$\Gamma^{(D)}_{ij} = \sum_{n=1}^{N} J^{(n)}(\omega_{ij})(1+\bar{n}_{\omega_{ij}})\left|S^{(n)}_{ij}\right|^2 \tag{9}$$

for the damping rates and

$$\Gamma^{(G)}_{ij} = \sum_{n=1}^{N} J^{(n)}(|\omega_{ij}|)\bar{n}_{|\omega_{ij}|}\left|S^{(n)}_{ij}\right|^2 \tag{10}$$

for the gain rates. $S^{(n)}_{ij} = \langle i|S^{(n)}|j\rangle$ are the matrix elements of the system's degrees of freedom in the energy basis. Finally, the diagonal elements are given by $\Gamma^{(0)}_i = -\sum_{j=1}^{i-1}\Gamma^{(D)}_{ji} - \sum_{j=i+1}^{d}\Gamma^{(G)}_{ji}$ for $1 < i < d$, $\Gamma^{(0)}_1 = -\sum_{j=2}^{d}\Gamma^{(G)}_{j1}$, and $\Gamma^{(0)}_d = -\sum_{j=1}^{d-1}\Gamma^{(D)}_{jd}$. Most importantly, rates $\Gamma^{(D)}_{ij}$ and $\Gamma^{(G)}_{ij}$ provide analytical expressions that show how the N local and independent system-reservoir couplings, as quantified by $J^{(n)}(\omega)$, can cause a block diagonal Λ, inducing broken ergodicity.

B. Pathways suppression for N spins-1/2

Let us first consider the scaling of pathways suppression for N spins-1/2 (where $N \geqslant 1$). We assume that H_S has nondegenerate gaps and that all its eigenstates are products of local states in a given direction (for instance, products of $\sigma^{(n)}_z$ eigenstates). Although this product-states assumption excludes spin chains of arbitrary longitudinal and transverse couplings, it includes Hamiltonians beyond Ising models, as in the cases of long-range interactions in the spin model for tertiary structures in protein folding [4] and of three-body interaction Hamiltonians on a lattice [41]. If each spin is coupled to an independent reservoir, we find that the minimum number of zeros, N_{zeros}, in matrix Λ is given by

$$N_{\text{zeros}} = 2^N[2^N - (N+1)]. \tag{11}$$

This can be technically understood by noticing that each line in Λ contains at most $N+1$ nonzero elements (N off-diagonal elements, since there are at most N spins to be flipped by a one-body operator $S^{(n)}$, plus the diagonal element, finite as long as there is at least one finite off-diagonal element in the same line). Hence, we find at least $2^N - (N+1)$ zeros

in each line of Λ. The number of lines is 2^N, explaining the result in N_{zeros}. For large spin-1/2 chains, $N \gg 1$, the minimum number of zeros approaches the number of matrix elements, 2^{2N}. The almost linear growth of the number of allowed relaxation pathways is, therefore, unable to ensue the exponential growth of the system dimension. It suggests that the kind of broken ergodicity we find in our model tends to be exponentially more likely to appear in larger spin chains.

IV. SPIN CHAINS OF $N = 2$ AND $N = 3$

In this section, we focus on specific examples of the interplay between frustration and inhomogeneous environments in the relaxation of spin chains. We choose the exactly solvable Ising model, as typically employed in frustration scenarios [2,3]. We restrict ourselves to case studies of small chains, which are more tractable analytically and provide clear examples of the relevant effects here. Our results are of especial interest to the context of quantum simulation [31,32,42,43], where the quantum dynamics of small open Ising chains can be tracked and controlled with high fidelity. Reference [31], in particular, pioneered the engineering of reservoirs for finite chains, going beyond the design of Hamiltonians in quantum simulation.

A. Relaxation of $N = 2$ frustrated homogeneously open Ising chain: A case for the microscopic model

Following through the discussion below Eq. (5), we bring here an example highlighting why the microscopic model is more appropriate to describe relaxation of a frustrated spin chain. We consider an Ising chain homogeneously coupled to the environment. We show that the microscopic model is consistent with standard statistical mechanics, namely, the steady state at $T \to 0$ is the ground state of the entire system. We also show that the phenomenological model contradicts such expectation.

The system Hamiltonian is described by

$$H_S = h_1\sigma_z^{(1)} + h_2\sigma_z^{(2)} + \Delta_{12}^{(A)}\sigma_z^{(1)}\sigma_z^{(2)}, \tag{12}$$

where $\sigma_z^{(n)}$ is the z-Pauli matrix of the nth spin-1/2. We choose $\Delta_{12}^{(A)} \gg h_1 > h_2 > 0$. The energy spectrum here is given by

$$\begin{aligned}
|1\rangle &= |\downarrow\uparrow\rangle, \quad E_1 = -\Delta_{12}^{(A)} - h_1 + h_2,\\
|2\rangle &= |\uparrow\downarrow\rangle, \quad E_2 = -\Delta_{12}^{(A)} + h_1 - h_2,\\
|3\rangle &= |\downarrow\downarrow\rangle, \quad E_3 = \Delta_{12}^{(A)} - h_1 - h_2,\\
|4\rangle &= |\uparrow\uparrow\rangle, \quad E_4 = \Delta_{12}^{(A)} + h_1 + h_2.
\end{aligned} \tag{13}$$

The ground state frustrates the term $h_2\sigma_z^{(2)}$ in H_S, in agreement with the formalism in Ref. [15]. We also choose H_S to be nondegenerate and all transition frequencies ω_{ij} to be unequal.

We are interested in energy-exchanging system-reservoir couplings, that satisfy $[H_S, S^{(n)}] \neq 0$. We assume that $S^{(n)} = \sigma_x^{(n)}$. We also choose the ohmic spectral function, $J^{(n)}(\omega) = \kappa^{(n)}\omega$, where $\kappa^{(n)}$ is a dimensionless parameter that we consider as a free variable.

When we set $\kappa^{(1)} = \kappa^{(2)}$ (homogeneous environment), the system finds a unique steady state, namely, the Gibbs state $\rho_S(\infty) = \exp(-\beta H_S)/Z_S$. At the zero-temperature limit,

$$\rho_S(\infty)|_{T\to 0} \to |1\rangle\langle 1| = |\downarrow\uparrow\rangle\langle\downarrow\uparrow|. \tag{14}$$

The phenomenological approach, as discussed above [see the paragraph below Eq. (5)], leads to the local ground state of each spin (as if they were uncoupled). The Lindbladian for this case (i.e., locally coupled to the environment via $\sigma_x^{(n)}$, at the zero-temperature limit, $T \to 0$) is

$$L^{(\text{ph})}[\rho_S] = \sum_{n=1,2} \gamma_n(\sigma_-^{(n)}\rho_S\sigma_+^{(n)} - \{\rho_S, \sigma_+^{(n)}\sigma_-^{(n)}\}/2), \tag{15}$$

where the decay rates are $\gamma_n = J^{(n)}(h_n) = \kappa^{(n)}h_n$ and the rising and lowering operators are the usual $\sigma_\pm^{(n)} = (\sigma_x^{(n)} \pm i\sigma_y^{(n)})/2$ (or, $\sigma_-^{(n)} = |\downarrow\rangle_n\langle\uparrow|_n$ and $\sigma_+^{(n)} = \sigma_-^{(n)\dagger}$). Equation (15) has been derived here from Eq. (4), by applying it first to $H_{S1}^{(\text{ph})} = h_1\sigma_z^{(1)}$, then to $H_{S2}^{(\text{ph})} = h_2\sigma_z^{(2)}$, and finally adding the two terms, as typically done in weak-coupling regimes [17]. This phenomenological Lindbladian, $L^{(\text{ph})}[\rho_S]$, leads to

$$\rho_S^{(\text{ph})}(\infty)|_{T\to 0} \to |\downarrow\downarrow\rangle\langle\downarrow\downarrow| = |3\rangle\langle 3|. \tag{16}$$

Equation (16) shows that the phenomenological model introduces here a spurious broken ergodicity, which is properly avoided by the microscopic description of this frustrated spin chain relaxation, as shown in Eq. (14). This comparison underlines that the microscopic model is more suitable for describing relaxation in spin chains, especially when frustration is present.

B. Relaxation of $N = 2$ unfrustrated inhomogeneously open Ising model

1. Blocked ground state

Our next step is to illustrate how a strongly inhomogeneously environment can break ergodicity in a unfrustrated spin chain. The system Hamiltonian is described by [see Fig. 2(a)]

$$H_S = h_1\sigma_z^{(1)} + h_2\sigma_z^{(2)} - \Delta_{12}^{(B)}\sigma_z^{(1)}\sigma_z^{(2)}, \tag{17}$$

where $\sigma_z^{(n)}$ is the z-Pauli matrix of the nth spin-1/2. We choose $h_1 > h_2 > \Delta_{12}^{(B)} > 0$, that guarantees the absence of energy frustration. We also choose H_S to be nondegenerate and all transition frequencies ω_{ij} to be unequal. The energy spectrum here reads

$$\begin{aligned}
|1\rangle &= |\downarrow\downarrow\rangle, \quad E_1 = -h_1 - h_2 - \Delta_{12}^{(B)},\\
|2\rangle &= |\downarrow\uparrow\rangle, \quad E_2 = -h_1 + h_2 + \Delta_{12}^{(B)},\\
|3\rangle &= |\uparrow\downarrow\rangle, \quad E_3 = h_1 - h_2 + \Delta_{12}^{(B)},\\
|4\rangle &= |\uparrow\uparrow\rangle, \quad E_4 = h_1 + h_2 - \Delta_{12}^{(B)}.
\end{aligned} \tag{18}$$

We still assume that $S^{(n)} = \sigma_x^{(n)}$ and that the spectral function is ohmic, $J^{(n)}(\omega) = \kappa^{(n)}\omega$.

In Fig. 2(b) dashed arrows indicate the relaxation pathways induced by the two independent baths, characterized by $\kappa^{(1)}$ and $\kappa^{(2)}$. Bath (1) induces, via $\sigma_x^{(1)}$, transitions $|1\rangle \leftrightarrow |3\rangle$ and $|2\rangle \leftrightarrow |4\rangle$. Bath (2) induces, via $\sigma_x^{(2)}$, transitions $|1\rangle \leftrightarrow |2\rangle$ and $|3\rangle \leftrightarrow |4\rangle$. If we make $\kappa^{(1)} = 0$ and $\kappa^{(2)} = 1$ (strongly inhomogeneous environment), subspace $\{|1\rangle, |2\rangle\}$ becomes decoupled from $\{|3\rangle, |4\rangle\}$. The system starting its dynamics

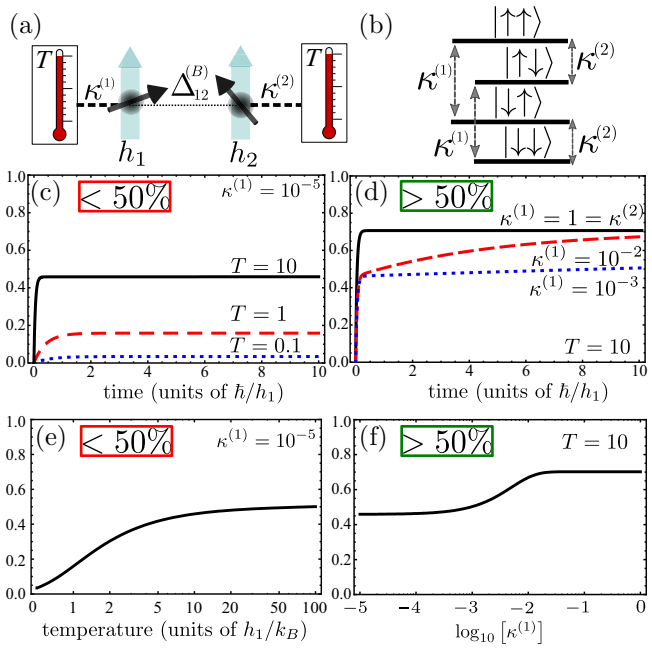

FIG. 2. Inhomogeneously open Ising chain simulates a protein denaturation experiment. (a) Ising chain of two spins ($N = 2$), black arrows represent $\sigma_z^{(n)}$. (b) Energy levels and relaxation pathways: vanishing $\kappa^{(1)}$ blocks low-energy subspace from high-energy subspace. (c) Excitation probability $P_{\rm exc}(t) = 1 - \langle 1|\rho_S(t)|1\rangle$ as a function of time t (units of $\hbar/h_1$) at fixed $\kappa^{(1)} = 10^{-5}$, for temperatures $T = 0.1h_1/k_B$ (dotted blue, lower curve), $T = 1h_1/k_B$ (dashed red, middle curve), and $T = 10h_1/k_B$ (solid black, upper curve). (d) Excitation probability $P_{\rm exc}(t) = 1 - \langle 1|\rho_S(t)|1\rangle$ as a function of time t (units of $\hbar/h_1$) at fixed temperature $T = 10h_1/k_B$, for $\kappa^{(1)} = 10^{-3}$ (dotted blue, lower curve), $\kappa^{(1)} = 10^{-2}$ (dashed red, middle curve), and $\kappa^{(1)} = 1 = \kappa^{(2)}$ (solid black, upper curve). (e) $P_{\rm exc}(t = 10)$ with respect to T (units of h_1/k_B) at fixed $\kappa^{(1)} = 10^{-5}$. (f) $P_{\rm exc}(t = 10)$ with respect to $\kappa^{(1)}$ at fixed $T = 10h_1/k_B$. We set $h_2 = h_1/2$, $\Delta_{12}^{(B)} = h_1/3$ and $\kappa^{(2)} = 1$. Panels (c)–(f) evidence that chemical-like excitations (by varying the coupling $\kappa^{(1)}$) exceed the 50% limit from thermal excitations at time $t = 10\hbar/h_1$. The higher chemical-like excitation (f) as compared to the thermal excitation (e) remarkably resembles the experimental results in Ref. [34] (see Fig. 4 in the Appendix).

at the highest energy subspace, $\{|3\rangle, |4\rangle\}$, gets blocked from attaining the lowest energy subspace, $\{|1\rangle, |2\rangle\}$. The strongly inhomogeneous environment induces broken ergodicity in the relaxation of an unfrustrated spin chain, in this case.

2. A simulation of protein denaturation

Proteins are relevant to the present discussion because they may be affected not only by frustration (as mentioned in the introduction) but also by spatially inhomogeneous environments. The spatial inhomogeneity of a protein's environment can lead to measurable differences between thermal and chemical denaturations [34,39,40]. We intend to simulate this feature of the protein dynamics, as inspired by Refs. [4,35]. More precisely, we look for simulating the experimental results reported in Ref. [34]. It should be emphasized that, rather than using open spin chains to realistically map the stochastic dynamics of aminoacid chains, our purpose here is to search for universal features appearing in the relaxation of inhomogeneously open chains. As a typical procedure, the experiment in Ref. [34] follows the state of the protein as a function of increasing temperature at a given chemical concentration, and compares it to the increase in the denaturant concentration at a constant temperature (see the Appendix for further discussion).

Here we follow a protocol analogous to that in Ref. [34]. We calculate the relaxation of our open Ising chain, Eq. (17). First, we set different temperatures T for a constant strongly inhomogeneous environment ($\kappa^{(1)} \ll \kappa^{(2)}$), to simulate thermal denaturation. Then we vary $\kappa^{(1)}$ [the coupling with bath (1)], at constant T and constant $\kappa^{(2)}$, to simulate the variation of solvent concentration in the protein environment. In Figs. 2(c) and 2(d), we show the excitation probability in time, defined here as $P_{\rm exc}(t) = 1 - \langle 1|\rho_S(t)|1\rangle$. To recall a protein-like denaturation dynamics, we start from our native-like state $|1\rangle$, hence $P_{\rm exc}(0) = 0$. Now we compare the two types of excitation processes in time ($\hbar/h_1$ units), i.e., the thermal versus the chemical-like. In the thermal excitation process, we let $\kappa^{(1)} = 10^{-5}$, $\kappa^{(2)} = 1$ and obtain $P_{\rm exc}(t)$ at temperatures $T = 0.1$ to 10 (h_1/k_B units). We set $h_2 = h_1/2$ and $\Delta_{12}^{(B)} = h_1/3$. We see a saturation $P_{\rm exc}(t) \lesssim 50\%$ at high temperatures. In the chemical-like excitation process, we keep the high temperature $T = 10$ and vary the coupling $\kappa^{(1)}$ from 10^{-3} to 1. We see the system crossing the 50% barrier and attaining higher excitations at higher couplings. Figure 2(e) shows $P_{\rm exc}(t = 10)$ as a function of T at $\kappa^{(1)} = 10^{-5}$. Because the system has effectively only two energy levels in the case $\kappa^{(1)} = 10^{-5}$, the maximal of $\partial_T P_{\rm exc}(t = 10)$ is around $T_\theta \sim 1$, near the peak of the specific heat, another typical signature of thermal denaturation of proteins. Figure 2(f) shows $P_{\rm exc}(t = 10)$ as a function of $\kappa^{(1)}$ at $T = 10$. The higher chemical-like excitation in Fig. 2(f) as compared to the thermal one in Fig. 2(e) remarkably resembles experimental results in Ref. [34] (see the Appendix).

Our formalism may be regarded as a generalization of the molecular transfer model, used for describing thermal and chemical denaturation in proteins [36–40]. The molecular transfer model combines coarse-grained molecular dynamics simulations and Tanford's transfer model [35] to accurately predict the dependence of equilibrium properties of proteins at finite concentration of osmolytes and denaturants. Tanford's model, the precursor, distinguishes those peptide groups that are in contact with the surrounding environment (solvent-accessible surface area) from those that are, by contrast, shielded from the solvent by other parts of the protein molecule. This inhomogeneous coupling to the environment consists in the working principle of Tanford's model to capture chemical denaturation. Despite acknowledging its practical success, we propose here a solution to an issue we find in the theoretical foundations of the molecular transfer model, namely, the unequal footing for treating thermal and chemical effects [39,40]. On the one hand, temperature enters in the *ad hoc* relaxation and diffusion rates of the Langevin equations describing the polymer stochastic dynamics. On the other hand, chemical effects enter in the free energies for the thermal equilibrium states of the protein transferred (hence the name) from a solution without solvent to another

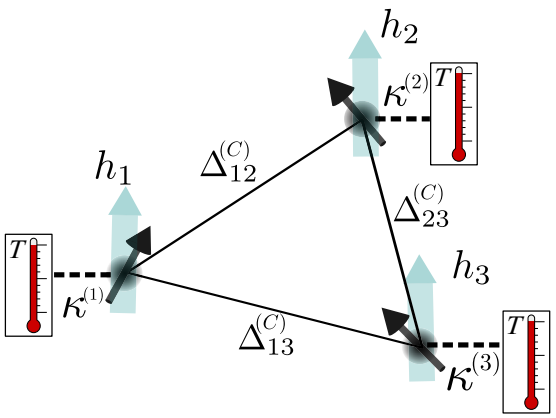

FIG. 3. Frustrated Ising chain in triangular lattice: $\Delta_{12}^{(C)} = \Delta > 0$ induces antiferromagnetism, whereas $\Delta_{23}^{(C)} = \Delta - \delta > 0$ and $\Delta_{13}^{(C)} = \Delta - 2\delta > 0$ induce ferromagnetism. We choose a perturbative external field $h_1 = h_2 = h_3 = h > 0$, where $h = 3\delta \ll \Delta$, to perturbatively break spectral degeneracies. The three reservoirs are independent, all set to temperature T. Again, each spin-reservoir coupling $\kappa^{(n)}$ is a free parameter. We show that an inhomogeneous environment ($\kappa^{(i)} \neq \kappa^{(j)}$, for $i \neq j$) can break ergodicity and select relaxation to a single state from the three lowest nearly degenerated eigenenergies (as induced by frustration).

with added solvent. We conjecture that our results provide the missing connection between this stochastic Langevin approach for describing thermal effects and the thermodynamic transfer model for describing chemical effects. Our hypothesis could be tested, for instance, by deriving bead-dependent and state-dependent friction coefficients [44,45] and random forces from a system-plus-reservoir approach, consistently with the time-dependent solvent-accessible surface area of the protein. Our conjecture could also be explored by further investigating polyelectrolyte conformations [46], where the spatial distribution of surrounding ions matters as much as their concentration to the polymer's shape. The study of inhomogeneous environments may also be relevant to the context of adsorption of flexible polymer chains on a surface [47], where the number of chain-surface contacts is variable.

C. Relaxation of $N = 3$ frustrated Ising model: Inhomogeneous environment mitigates frustration

A typical model in frustration studies is the disordered Ising model in a triangular lattice (see Sec. 2.5 of Ref. [1]), that we illustrate in Fig. 3. If two couplings tend to align spins to the same direction (ferromagnetic), but the other to the opposite direction (antiferromagnetic), then each spin will frustrate the minimization of at least one energetic contribution. Our goal here is to search, in this paradigmatic example, whether an inhomogeneous environment can suppress the dynamical effects induced by frustration, providing the opposite effect from the $N = 2$ case above (where an inhomogeneous environment was able to introduce a frustration-like effect in an unfrustrated spin chain).

The Hamiltonian in this case is set to $H_S = H_0 + V$, where

$$H_0 = \Delta_{12}^{(C)}\sigma_z^{(1)}\sigma_z^{(2)} - \Delta_{23}^{(C)}\sigma_z^{(2)}\sigma_z^{(3)} - \Delta_{13}^{(C)}\sigma_z^{(1)}\sigma_z^{(3)} \quad (19)$$

and $V = h_1\sigma_z^{(1)} + h_2\sigma_z^{(2)} + h_3\sigma_z^{(3)}$. We select $h_1 = h_2 = h_3 \equiv h > 0$, $\Delta_{12}^{(C)} = \Delta$, $\Delta_{23}^{(C)} = \Delta - \delta$, and $\Delta_{13}^{(C)} = \Delta - 2\delta$. We choose the external field to be perturbative, $h \ll \Delta$, and fix $h = 3\delta$, so to perturbatively break degeneracies. The spectrum of H_S here is

$$\begin{aligned}
|1\rangle &= |\downarrow\downarrow\downarrow\rangle, \quad E_1 = -\Delta - 6\delta,\\
|2\rangle &= |\uparrow\downarrow\downarrow\rangle, \quad E_2 = -\Delta - 4\delta,\\
|3\rangle &= |\downarrow\uparrow\downarrow\rangle, \quad E_3 = -\Delta - 2\delta,\\
|4\rangle &= |\downarrow\uparrow\uparrow\rangle, \quad E_4 = -\Delta + 2\delta,\\
|5\rangle &= |\uparrow\downarrow\uparrow\rangle, \quad E_5 = -\Delta + 4\delta,\\
|6\rangle &= |\uparrow\uparrow\uparrow\rangle, \quad E_6 = -\Delta + 12\delta,\\
|7\rangle &= |\downarrow\downarrow\uparrow\rangle, \quad E_7 = 3\Delta - 6\delta,\\
|8\rangle &= |\uparrow\uparrow\downarrow\rangle, \quad E_8 = 3\Delta. \qquad (20)
\end{aligned}$$

Note that states $|1\rangle$, $|2\rangle$, and $|3\rangle$, respectively, frustrate the terms $\propto \Delta_{12}^{(C)}$, $\Delta_{13}^{(C)}$, and $\Delta_{23}^{(C)}$. In this example, we find many degenerate gaps (e.g., $E_2 - E_1 = E_3 - E_2 = E_5 - E_4$). However, in the present example, no gap degeneracy affects any of the results discussed in this section. That is because, at given (n) and ω [see $A_\omega^{(n)}$ in Eq. (5)], the matrix element $\langle i|S^{(n)}|j\rangle$ is nonzero for at most one transition $|i\rangle \to |j\rangle$, where we use $S^{(n)} = \sigma_x^{(n)}$. We also keep using an ohmic spectral function, $J^{(n)}(\omega) = \kappa^{(n)}\omega$.

Let us compare four scenarios, all starting from the most excited state, $\rho_S(0) = |8\rangle\langle 8|$. For the sake of having a clear picture, we keep in mind, in all cases, the very low temperature limit, $k_BT \approx \delta \ll \Delta$.

Case 1. Homogeneous environment: $\kappa^{(1)} = \kappa^{(2)} = \kappa^{(3)} = 1$. In the $t \to \infty$ limit, we find that the system reaches thermal equilibrium. The Gibbs state $\rho_S(\infty) = \exp(-\beta H_S)/Z_S$ is the unique solution here. At low temperatures, $k_BT \approx \delta \ll \Delta$, the three most populated states are, of course, $|1\rangle$, $|2\rangle$, and $|3\rangle$.

Case 2. Inhomogeneous environment I: $\kappa^{(1)} = \kappa^{(2)} = 1$ and $\kappa^{(3)} = 0$. Here we find broken ergodicity, so the system gets trapped in the subspace $\{|1\rangle, |2\rangle, |3\rangle, |8\rangle\}$. In the $t \to \infty$ limit, at low temperatures, $k_BT \approx \delta \ll \Delta$, the three most populated states are also $|1\rangle$, $|2\rangle$, and $|3\rangle$. This inhomogeneous environment, at low temperatures, does not dramatically change the results found in the homogeneous case.

Case 3. Inhomogeneous environment II: $\kappa^{(1)} = 1, \kappa^{(2)} = 0$, and $\kappa^{(3)} = 1$. Here we find broken ergodicity, so the system gets trapped in the subspace $\{|3\rangle, |4\rangle, |6\rangle, |8\rangle\}$. In the $t \to \infty$ limit, at low temperatures, $k_BT \approx \delta \ll \Delta$, the most populated state is $|3\rangle$. Remarkably, the populations of states $|1\rangle$ and $|2\rangle$ precisely vanish, $\langle 1|\rho_S(\infty)|1\rangle = \langle 2|\rho_S(\infty)|2\rangle = 0$, at any temperature.

Case 4. Inhomogeneous environment III: $\kappa^{(1)} = 0$ and $\kappa^{(2)} = \kappa^{(3)} = 1$. Here we find broken ergodicity, so the system gets trapped in the subspace $\{|2\rangle, |5\rangle, |6\rangle, |8\rangle\}$. In the $t \to \infty$ limit, at low temperatures, $k_BT \approx \delta \ll \Delta$, the most populated state is $|2\rangle$. Remarkably, the populations of $|1\rangle$ and $|3\rangle$ precisely vanish, $\langle 1|\rho_S(\infty)|1\rangle = \langle 3|\rho_S(\infty)|3\rangle = 0$, at any temperature.

We find that, in cases 3 and 4 above, the inhomogeneous environments have strongly inhibited the thermal-like distribution of the three nearly degenerated lowest-energy states.

Rather, they have isolated a single state to play the role of an effective ground state ($|3\rangle$ in case 3 and $|2\rangle$ in case 4). This shows how an inhomogeneous environment can suppress the effect of frustration, here represented by the (approximate) degeneracy of the low-energy levels. In the context of quantum simulation [31,32,42,43], inhomogeneous environments may serve in the preparation of specific target states.

V. CONCLUSIONS

We employed a system-plus-reservoir approach to investigate how strongly inhomogeneous environments compete with frustration in the relaxation of finite open chains with Ising-type interactions. The system-plus-reservoir approach allowed us to address frustration and dissipation in a consistent manner. We derived a Markovian quantum master equation for a generic chain within the microscopic model, valid in the ultrastrong intrachain couplings regime, going beyond phenomenological models. In Sec. III we established a sufficient condition for our inhomogeneous environments to break ergodicity in a general chain, namely, to have a block diagonal Λ. We have explicitly derived Λ_{ij} in Eqs. (8)–(10) and discussed its minimum number of zeros for the case of N spins-1/2 in Eq. (11). In Sec. IV A we found an example that highlights the relevance of the microscopic model to properly describe relaxation in the presence of frustration, showing how to avoid a spurious broken ergodicity from the phenomenological model. In Sec. IV B we examined a scenario where the strong inhomogeneity of the environment caused broken ergodicity in an unfrustrated spin chain. This example allowed us to simulate the results from a recent experiment on the difference between thermal and chemical protein denaturation, where environment inhomogeneity is also key. In Sec. IV C we found that inhomogeneous environments can suppress the effect of frustration in the relaxation of the paradigmatic frustrated spin chain in a triangular lattice. More precisely, in two of the studied cases, the inhomogeneous environment has strongly inhibited the thermal-like distribution of the three nearly-degenerated lowest-energy states, by isolating a single state as an effective ground state.

Our fundamental study on relaxation of open chains with Ising-type interactions, subjected to inhomogeneous environments and to frustration, suggests promising perspectives for applying state-of-the-art quantum simulators [31,32,42,43] to investigate the dissipative dynamics of proteins, especially denaturation [34,37–40], of polyelectrolytes [46], as well as of polymers adsorption [47]. This would mean going beyond the already formidable task of using quantum annealers to calculate the (equilibrium) folded state of a protein [48,49]. The role of the competition between frustration (Hamiltonian contribution) and inhomogeneous environments (dissipative contribution) could possibly find applications also in the context of driven-dissipative phase transitions [32].

ACKNOWLEDGMENTS

We thank P. H. L. Martins for stimulating comments. D.V. and T.W. acknowledge support from Instituto Nacional de Ciência e Tecnologia de Informação Quântica, Brazil.

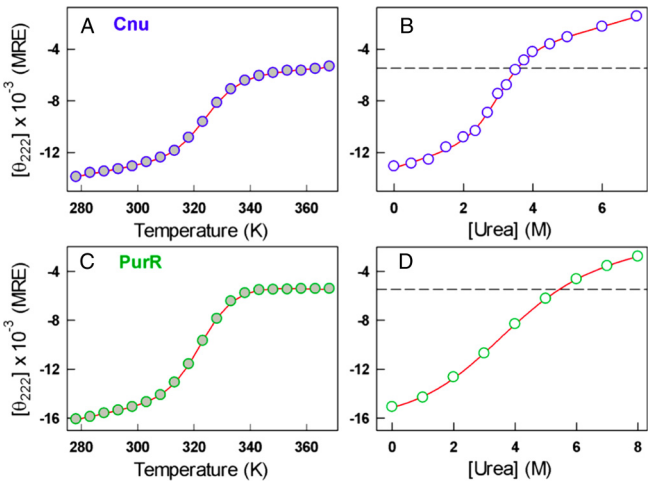

FIG. 4. *Reprint of Fig. 1 from A. Narayan, K. Bhattacharjee, and A. N. Naganathan, Biochemistry* **58**, *2519 (2019), under CC-BY License* (Ref. [34]). Original caption: Thermal (filled circles, panels A and C) and chemical unfolding (empty circles and at 298 K, panels B and D) curves of Cnu at pH 5.0 (blue) and PurR at pH 7.0 (green) monitored by far-UV CD at 222 nm and reported in MRE units (degrees square centimeters per decimole). Dashed lines in panels B and D represent the highest-temperature far-UV CD signal. Red curves are fits to two-state models.

APPENDIX: PROTEIN DENATURATION EXPERIMENT FROM REF. [34] REFERRED TO IN SEC. IV B 2

We reprint here part of the results published under CC-BY License by A. Narayan, K. Bhattacharjee and A. N. Naganathan in *Biochemistry* **58**, 2519 (2019), our Ref. [34]. The paper, "Thermally versus chemically denatured protein states," is crucial to our results in Sec. IV B 2.

Figure 4 describes an experiment on the differences in conformational preferences of thermally and chemically denatured protein states [34]. The authors employ a spectroscopic technique known as far-ultraviolet (far-UV) circular dichroism (CD), that reveals the local conformational (angular) preference of peptide bonds. They use thermal denaturation data of Cnu, a bacterial nanosensor of environmental conditions, as well as of PurR, a member of the LacI DNA-binding domain family, with which they compare their chemical denaturation results. CD signals are reported in degrees square centimeters per decimole (MRE units). The results are independent of protein concentration, protein length, and slight differences in sample path length, as tested with the purpose of eliminating ambiguities on the origins of the observed effect.

Key to the present paper, Fig. 4 shows that the increase of urea concentration in the protein's environment opens excitation pathways that are otherwise unavailable. Urea allows the protein to achieve denatured states that cannot be accessed solely by thermal means. By increasing the temperature without urea (panels A and C, the system's response abruptly changes (around 320–330 K) from a native (folded) state to a denatured (unfolded) state, approximately saturating at a certain high-temperature plateau dashed lines in panels B and D. The addition of urea at constant temperature (panels B and

D breaks this thermal saturation and causes the data to clearly exceed the plateau, even at a relatively low temperature with respect to thermal denaturation (298 K).

Remarkably similar behavior has been shown in our Sec. IV B 2, with a two-spin-1/2 chain inhomogeneously open to the environment. A strongly inhomogeneous environment ($\kappa^{(1)} \ll \kappa^{(2)} = 1$) induced a plateau in the thermal excitation of the chain [see Fig. 2(e)]. This plateau was broken by the increase in $\kappa^{(1)}$, which played the role in our model of a chemical concentration in the system's environment. The idea was that the larger the chemical concentration, the more homogeneous we expect the system's environment to be, hence the closest $\kappa^{(1)} \approx \kappa^{(2)}$ [see Fig. 2(f)]. Our results suggest that the differences between thermal and chemical denaturation in proteins can be regarded as a more general problem of how ergodicity depends on the inhomogeneity of system-environment couplings, generalizing the molecular transfer model [39] as explained in Sec. IV B 2.

[1] K. H. Fischer and J. A. Hertz, *Spin Glasses* (Cambridge University Press, Cambridge, 1991).
[2] S. F. Edwards and P. W. Anderson, J. Phys. F: Metal Phys. **5**, 965 (1975).
[3] D. Sherrington and S. Kirkpatrick, Phys. Rev. Lett. **35**, 1792 (1975).
[4] J. D. Bryngelson and P. G. Wolynes, Proc. Natl. Acad. Sci. USA **84**, 7524 (1987).
[5] F. O. Tzula, D. Vasilchuk, and G. I. Makhatadze, Proc. Natl. Acad. Sci. USA **114**, E1627 (2017).
[6] K. A. Dill and H. S. Chan, Nat. Struct. Biol. **4**, 10 (1997).
[7] Z. Yan and J. Wang, Phys. Rev. Lett. **122**, 018103 (2019).
[8] W. Bialek, *Biophysics: Searching for Principles* (Princeton University Press, Princeton, 2012).
[9] A. H. Castro Neto, E. Novais, L. Borda, G. Zaránd, and I. Affleck, Phys. Rev. Lett. **91**, 096401 (2003).
[10] E. Novais, A. H. Castro Neto, L. Borda, I. Affleck, and G. Zaránd, Phys. Rev. B **72**, 014417 (2005).
[11] M. Znidaric, T. Prosen, G. Benenti, G. Casati, and D. Rossini, Phys. Rev. E **81**, 051135 (2010).
[12] M. Znidaric, Phys. Rev. E **92**, 042143 (2015).
[13] V. Yu. Shishkov, E. S. Andrianov, A. A. Pukhov, A. P. Vinogradov, and A. A. Lisyansky, Phys. Rev. E **98**, 022132 (2018).
[14] K. Wang, F. Piazza, and D. J. Luitz, Phys. Rev. Lett. **124**, 100604 (2020).
[15] S. M. Giampaolo, G. Gualdi, A. Monras, and F. Illuminati, Phys. Rev. Lett. **107**, 260602 (2011).
[16] N. Kellermann, M. Schmidt, and F. M. Zimmer, Phys. Rev. E **99**, 012134 (2019).
[17] H. P. Breuer and F. Petrucionne, *The Theory of Open Quantum Systems* (Oxford University Press, Oxford, 2002).
[18] A. O. Caldeira, *An Introduction to Macroscopic Quantum Phenomena and Quantum Dissipation* (Cambridge University Press, Cambridge, 2014).
[19] V. Weisskopf, Naturwissenschaften **23**, 631 (1935).
[20] A. O. Caldeira and A. J. Leggett, Ann. Phys. **149**, 374 (1983).
[21] D. Valente, J. Suffczyński, T. Jakubczyk, A. Dousse, A. Lemaître, I. Sagnes, L. Lanco, P. Voisin, A. Auffèves, and P. Senellart, Phys. Rev. B **89**, 041302(R) (2014).
[22] M. Michel, J. Gemmer, and G. Mahler, Eur. Phys. J. B **42**, 555 (2004).
[23] A. Levy and R. Kosloff, Europhys. Lett. **107**, 20004 (2014).
[24] T. Werlang, M. A. Marchiori, M. F. Cornelio, and D. Valente, Phys. Rev. E **89**, 062109 (2014).
[25] T. Werlang and D. Valente, Phys. Rev. E **91**, 012143 (2015).
[26] K. Joulain, J. Drevillon, Y. Ezzahri, and J. Ordonez-Miranda, Phys. Rev. Lett. **116**, 200601 (2016).
[27] F. Barra, Sci. Rep. **5**, 14873 (2015).
[28] E. Pereira, Phys. Rev. E **97**, 022115 (2018).
[29] G. De Chiara, G. Landi, A. Hewgill, B. Reid, A. Ferraro, A. J. Roncaglia, and M. Antezza, New J. Phys. **20**, 113024 (2018).
[30] E. Pereira, Phys. Rev. E **83**, 031106 (2011).
[31] J. T. Barreiro, M. Müller, P. Schindler, D. Nigg, T. Monz, M. Chwalla, M. Hennrich, C. F. Roos, P. Zoller, and R. Blatt, Nature (London) **470**, 486 (2011).
[32] M. Müller, S. Diehl, G. Pupillo, and P. Zoller, Adv. At. Mol. Opt. Phys. **61**, 1 (2012).
[33] V. Balachandran, G. Benenti, E. Pereira, G. Casati, and D. Poletti, Phys. Rev. Lett. **120**, 200603 (2018).
[34] A. Narayan, K. Bhattacharjee, and A. N. Naganathan, Biochemistry **58**, 2519 (2019).
[35] C. Tanford, J. Am. Chem. Soc. **86**, 2050 (1964).
[36] E. P. O'Brien, G. Ziv, G. Haran, B. R. Brooks, and D. Thirumalai, Proc. Natl. Acad. Sci. USA **105**, 13403 (2008).
[37] D. Thirumalai, E. P. O'Brien, G. Morrison, and C. Hyeon, Annu. Rev. Biophys. **39**, 159 (2010).
[38] J. L. England and G. Haran, Annu. Rev. Phys. Chem. **62**, 257 (2011).
[39] C. Hyeon and D. Thirumalai, Nat. Commun. **2**, 487 (2011).
[40] Z. Liu, G. Reddy, and D. Thirumalai, J. Phys. Chem. B **120**, 8090 (2016).
[41] B. Subramanian and J. Lebowitz, J. Phys. A: Math. Gen. **32**, 6239 (1999).
[42] J. Simon, W. S. Bakr, R. Ma, M. E. Tai, P. M. Preiss, and M. Greiner, Nature (London) **472**, 307 (2011).
[43] H. Schwager, J. I. Cirac, and G. Giedke, Phys. Rev. A **87**, 022110 (2013).
[44] G. Hummer, New J. Phys. **7**, 34 (2005).
[45] H. Yang, P. Bandarkar, R. Horne, V. B. P. Leite, J. Chahine, and P. C. Whitford, J. Chem. Phys. **151**, 085102 (2019).
[46] S. N. Innes-Gold, P. A. Pincus, M. J. Stevens, and O. A. Saleh, Phys. Rev. Lett. **123**, 187801 (2019).
[47] P. H. L. Martins, J. A. Plascak, and M. Bachmann, J. Chem. Phys. **148**, 204901 (2018).
[48] A. Perdomo, C. Truncik, I. Tubert-Brohman, G. Rose, and A. Aspuru-Guzik, Phys. Rev. A **78**, 012320 (2008).
[49] A. Perdomo-Ortiz, N. Dickson, M. Drew-Brook, G. Rose, and A. Aspuru-Guzik, Sci. Rep. **2**, 571 (2012).